Talanta 104 (2013) 219–227

Contents lists available at SciVerse ScienceDirect

Talanta

journal homepage: www.elsevier.com/locate/talanta

# Structural, morphological and sensing properties of layered polyaniline nanosheets towards hazardous phenol chemical

Hyung-Kee Seo [a,1], Sadia Ameen [b,1], M. Shaheer Akhtar [c,1], Hyung Shik Shin [b,*]

[a] Department of Chemistry, Colorado State University, Fort Collins, Colorado 80523-1872, USA
[b] Energy Materials & Surface Science Laboratory, Solar Energy Research Center, School of Chemical Engineering, Chonbuk National University, Jeonju 561-756, Republic of Korea
[c] New & Renewable Energy Material Development Center (NewREC), Chonbuk National University, Jeonbuk, Republic of Korea

ARTICLE INFO

*Article history:*
Received 15 September 2012
Received in revised form
17 October 2012
Accepted 18 October 2012
Available online 20 November 2012

*Keywords:*
Layered nanosheets
*I–V* characteristics
Phenol
Chemical sensor
Electrochemical impedance spectroscopy

ABSTRACT

Reliable sensing properties towards hazardous phenol chemical were detected by the novel working electrode of layered polyaniline (PANI) nanosheets. The layered PANI nanosheets were synthesized by the chemical polymerization of aniline monomer in the presence of hydrochloric acid and ammonium persulphate at 5 °C. The morphological, structural, optical, electrical and electrochemical properties of layered PANI nanosheets were extensively studied. The electrochemical behavior of layered PANI nanosheets based electrode was demonstrated by the electrochemical impedance spectroscopy (EIS) and cyclovoltametry (CV) measurements. The layered PANI nanosheets electrode showed reasonably good electrocatalytic activity towards the detection of phenol chemical, which resulted from the high redox current and low $R_{CT}$. The current–voltage (*I–V*) characteristics were used to elucidate the sensing parameters of the fabricated phenol chemical sensor with layered PANI nanosheets electrode. The fabricated phenol chemical sensor with layered PANI nanosheets electrode significantly attained the high sensitivity of ~1485.3 μA $mM^{-1}$ $cm^{-2}$ and the detection limit of ~4.43 μM with correlation coefficient (*R*) of ~0.9981 and short response time (10 s).



## 1. Introduction

Phenol and phenolic compound are widely used chemicals in plastics, fertilizers, paints, rubber, adhesives, paper and soap industries [1]. It is also used as an antiseptic, a topical anesthetic for sore throat lozenges and sprays as a skin exfoliant [2]. The excess concentration of phenol and phenolic compounds is an issue of environmental concern due to their toxicity and persistence or high adsorptive nature in the environment [3]. Phenol if ingested in excess by human body could cause nausea, vomiting, sweating, diarrhea, excessive salivation and headache [4]. The acute exposure to phenol and its derivatives might also cause gastrointestinal irritation, cardiovascular, central nervous system and respiratory effects [2,5]. The detection, identification and the quantification of phenol and its compounds are very important for clean environment. For the detection of phenol, several analytical techniques like gas chromatography [6], high performance liquid chromatography [7], capillary electrophoresis [8] and spectrophotometry [9] are used so far. The major drawbacks of these analysis methods are time-consuming, complex to perform and not easy to operate under in-situ monitoring which limits the practical applications. Electrochemical methods are the most adopted technique due to the advantages associated with its high sensitivity, greater selectivity, time efficiency, and reproducibility [10].

A unique organic p-type semiconductor polymer, polyaniline (PANI) is highly searched polymer due to its unique acid–base chemistry, stable electrical conduction, high-environmental stability and ease of fabrication [11–13]. Importantly, PANI possesses the typical conjugated bonds in the polymer skeleton which could be responsible for the charge conduction due to the generation of polarons or bipolarons [14]. The variable conductivity makes PANI as promising material for the specific application of electronics, optoelectronic, electrochemical, electrochromic, photovoltaic and sensing devices [15]. Moreover, the presence of the reactive –NH- groups in the polymer chain (PANI), positioned on either side by phenylene rings imparts the chemical flexibility to the system and improves the processibility to a large extent. PANI nanomaterial shows the versatility of nanostructures in the form of nanofibers, nanorods, nanowires and nanoflakes with high surface/volume ratio and low diffusional resistance [16]. Various PANI nanostructures display the improved optical, structural, electronic and electrical properties which might act as useful candidate for the application in electrochemical, electrochromic, biosensors and chemical sensors devices [17–18]. Recently, PANI nanomaterials have gained a great attention in the field of sensors including gas sensor, biosensor and chemical sensors [19]. In context of PANI based sensors, Kukla et al. prepared PANI thin films for detecting ammonia [20].

* Corresponding author. Fax: +82 63 270 2306.
*E-mail address:* hsshin@jbnu.ac.kr (H.S. Shin).
[1] Authors contributed equally to this work.

0039-9140/$ - see front matter © 2012 Elsevier B.V. All rights reserved.
http://dx.doi.org/10.1016/j.talanta.2012.10.089

Bo et al. explained the electrochemical DNA biosensor by PANI nanowires modified graphene electrode [21]. Recently, Kunzo et al. fabricated the hydrogen sensor based on unique oxygen plasma treated PANI thin film [22]. Till date, very few reports are available on phenol sensor using PANI nanomaterials. An amperometric phenol biosensor based on PANI electrode was studied in the aspects of optical and electrochemical properties [23]. Zhang et al. designed the composite electrode of PANI-ionic liquid-carbon nanofiber for the fabrication of highly sensitive amperometric biosensors towards phenols [24]. To the best of our knowledge, for the first time the layered PANI nanosheets based electrodes are used as an effective chemical sensor towards the efficient detection of phenol. In this paper, the layered PANI nanosheets have been synthesized through the chemical polymerization and applied directly for the fabrication of phenol chemical sensor. The fabricated phenol sensor based on layered PANI nanosheets exhibit a high sensitivity of $\sim$1485.3 μA $mM^{-1}$ $cm^{-2}$ and very low detection limit of $\sim$4.43 μM with correlation coefficient ($R$) of $\sim$0.9981 and short response time (10 s).

## 2. Experimental

### 2.1. Synthesis of layered PANI nanosheets

For the layered PANI nanosheets, the mixture of 0.1 mol of aniline monomer (Sigma-Aldrich, $\geq$99.5%) and 0.5 mol hydrochloric acid (HCl, Daejung Chemicals, Assay 35–37%) was dissolved in 150 ml deionized (DI) water and stirred for 15 min. The mixture was heated to 60 °C under constant stirring and later, 0.1 mol ammonium persulphate (APS, Sigma-Aldrich, $\geq$98%) was quickly added. Thereafter, the entire reaction mixture was immediately placed on an ice bath and maintained at the temperature of $\sim$5 °C for 6–8 h under static condition. After completion of the reaction, the greenish blue color precipitate was obtained. The precipitate was filtered and washed with copious amount of DI water and dried under vacuum for 24 h to obtain greenish-blue layered PANI nanosheets.

### 2.2. Characterization of layered PANI nanosheets

The morphological observations were studied by using field emission scanning electron microscopy (FESEM, Hitachi S-4700, Japan), the transmission electron microscopy (TEM, JEM-2010-JEOL, Japan) and the atomic force spectroscopy (AFM, Nanoscope IV, Digital Instruments, Santa Barbara, USA). The line scan element mapping was analyzed by the FESEM coupled Energy dispersive X-rays spectroscopy with the mapping mode. The structural modifications of the layered PANI nanosheets were studied by the Fourier transform infrared (FTIR; Nicolet, IR300), Raman scattering (Raman microscope, Renishaw) and X-rays diffraction (XRD, Rigaku, Cu Kα, $\lambda$=1:54178 Å) spectroscopy. The optical properties were measured by UV–vis spectrophotometer (JASCO, V-670, Japan) and the photoluminescence (PL) spectrum of layered PANI nanosheets was obtained with FluoroMax-2 Jobin-Yvon Spex Fluorometer (S.A. Inc.) with the excitation at $\sim$320 nm. The electrochemical behavior of layered PANI nanosheets based electrode was studied by the cyclic voltammetry (CV), using the WPG100 electrochemical measurement system. The CV was performed in a three-electrode one compartment cell using layered PANI nanosheets as working electrode, Pt wire as counter electrode and an Ag/AgCl reference electrode. Electrochemical impedance (EIS) measurements were carried out by two probes electrochemical system using layered PANI nanosheets electrode as working and Pt wire electrode as cathode in PBS solution with different concentration of phenol by applying 10 mV ac signal over the frequency range of 100 kHz–1 Hz using VersaSTAT4.

### 2.3. Fabrication and characterization of phenol chemical sensor using layered PANI nanosheets electrode

The electrode was prepared by compressing the finely grounded layered PANI nanosheets powder under a pressure of $\sim$6.6 t to form the pellets. The contacts were made by attaching the thin Cu wire on the pellet with the silver paste. Afterward, PANI electrode was subjected to drying at 60 $\pm$ 5 °C for 5–6 h in an oven under $N_2$. The phenol sensing performance was determined by simple two electrode current–voltage ($I$–$V$) characteristics (Electrometer, Keithley, 6517 A, USA), in which the layered PANI nanosheets pellet based electrode was used as working electrode and Pt wire as a counter electrode. A fixed amount of 0.1 M phosphate buffer solution (PBS, 10.0 ml) and the wide range of phenol concentrations from 20 μM–0.32 mM were used for the determination of sensitivity. The sensitivity of the fabricated phenol chemical sensor was estimated from the slope of the current versus concentrations from the calibration plot divided by the value of active area of sensor/electrode. The current response was measured from 0 V–2 V while the response time was measured as 10 s.

## 3. Results and discussion

### 3.1. Morphological characterizations of layered PANI nanosheets

Fig. 1 shows the FESEM and TEM images of layered PANI nanosheets. At low resolution (Fig. 1(a,b)), the synthesized PANI displays the uniform and compact layered sheets like morphology. The layered PANI nanosheets exhibit the average thickness of several hundred nanometers, as shown in Fig. 1(c). The morphology of the synthesized PANI is further characterized by TEM analysis, as depicted in Fig. 1(d). The layered morphology of PANI nanosheets is clearly visible which is similar to the FESEM results. There is no deformation of the morphology of layered PANI nanosheets under the high electron beam of TEM, suggesting the stability of the synthesized layered PANI nanosheets.

Fig. 2 shows the topographic and three dimensional (3D) AFM images of layered PANI nanosheets. The layered morphology of the synthesized PANI is visibly recorded in the topographic mode, as shown in Fig. 2(a). The 3D AFM image (Fig. 2(b)) has confirmed the same layered morphology, as detected in the topographic mode. The roughness of layered PANI nanosheets is estimated from AFM images by taking the value of the root mean roughness ($R_{rms}$). The layered PANI nanosheets exhibit relatively the high roughness of $\sim$52.3 nm. It is known that the electrode materials with large roughness factor display higher electrochemical behavior or the electrocatalytic activity [25]. The high roughness of layered PANI nanosheets might improve the electrochemical behavior towards the detection of phenol.

Fig. 3(a) shows the X-rays diffraction (XRD) patterns of layered PANI nanosheets. Typically, two diffraction peaks at 19.3° and 25.1° are recorded, corresponding to the periodicity parallel and perpendicular to the polymer chain, respectively. These peaks are also assigned to emeraldine structure of PANI. The recorded XRD patterns are similar to PANI sheets or matrix [25]. The element composition of the layered PANI nanosheets is analyzed by taking the line scan element mapping through EDS. Fig. 3(b, c) shows the line scan element mapping image and pie profile of the elements. The C and N elements are majorly distributed in the line scan mapping however, the traces of Cl and S elements are also detected, as seen in the corresponding pie bar graph as shown in Fig. 3(c). The uniform distribution of C and N elements confirm the formation of layered PANI nanosheets.

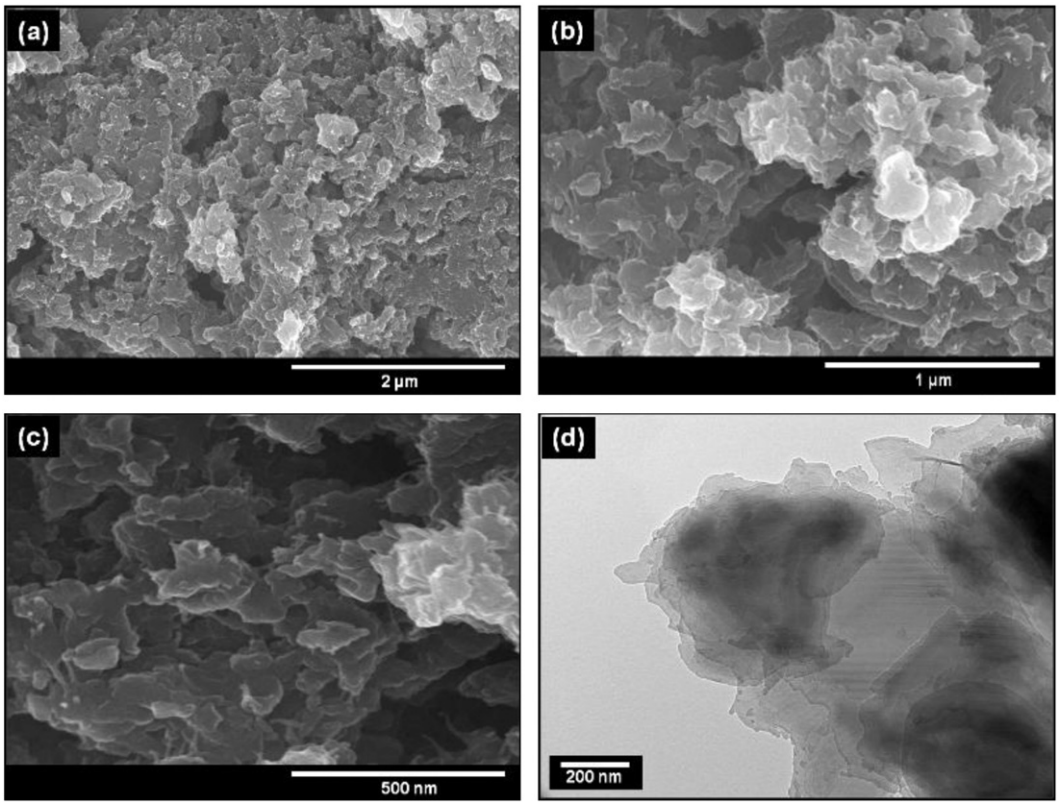


**Fig. 1.** FESEM images at different magnifications (a–c) and TEM image (d) of layered PANI nanosheets.

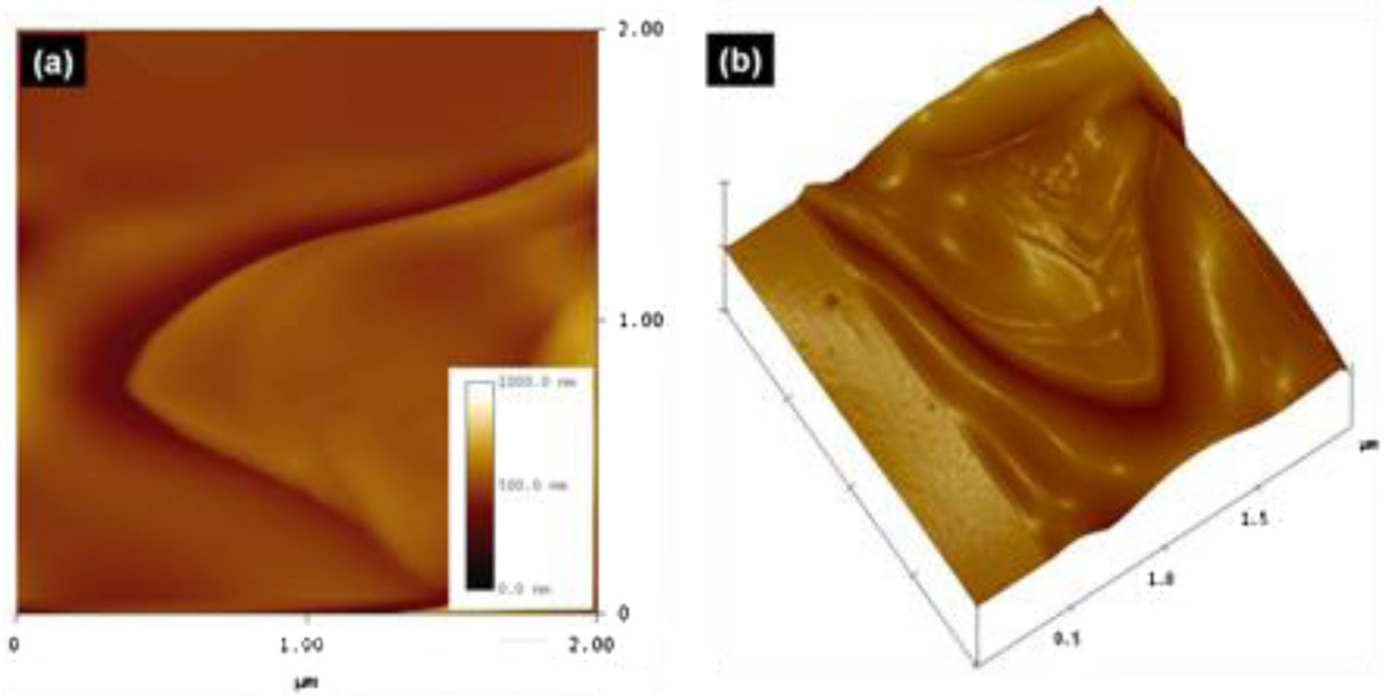


**Fig. 2.** Topographic (a) and three dimensional (b) AFM images of layered PANI nanosheets.

### *3.2. Structural and optical characterizations of layered PANI nanosheets*

Fig. 4 shows the FTIR spectrum of layered PANI nanosheets. The IR characteristic peaks at $\sim$1574 $cm^{-1}$, $\sim$1484 $cm^{-1}$, $\sim$1298 $cm^{-1}$ and $\sim$1106 $cm^{-1}$ (Fig. 4(a,b)) are observed in layered PANI nanosheets which represent the C=C stretching mode of the quinoid rings, C=C stretching mode of benzenoid rings, C–N stretching mode and N=Q=N (where Q represents the quionoid ring) stretching respectively. However, the appearance of the peak at

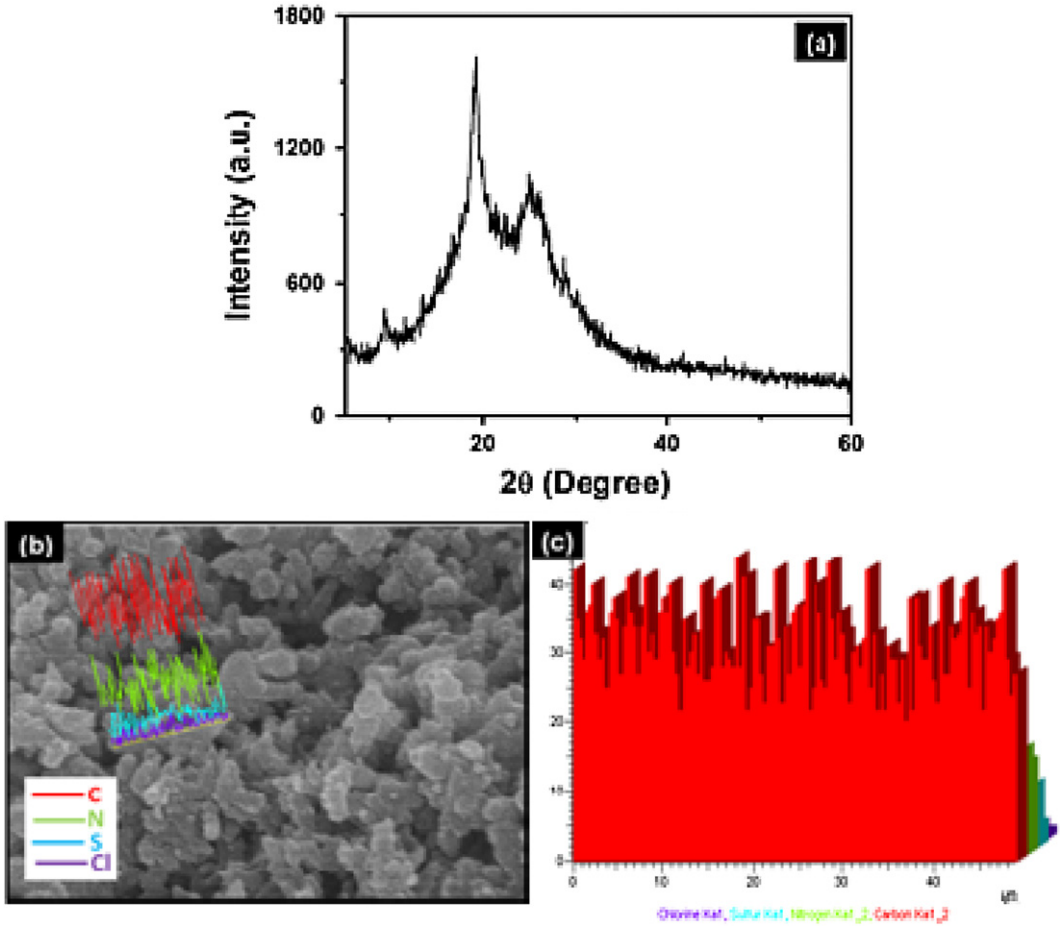


**Fig. 3.** (a) XRD patterns, (b) line scanning elemental mapping image and (c) the corresponding pie bar graph of layered PANI nanosheets.

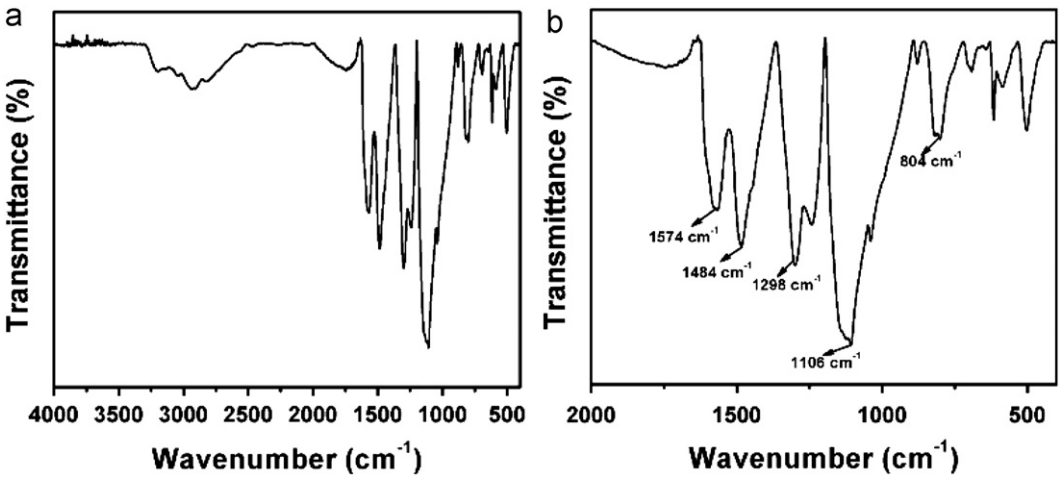


**Fig. 4.** FTIR spectra in the wavenumber range of (a) 4000–400 $cm^{-1}$ and (b) 2000–400 $cm^{-1}$ of layered PANI nanosheets.

$\sim$804 $cm^{-1}$ is associated to C–H bending out of the plane vibration of the benzene ring [26] and the broader IR peak at $\sim$3154 $cm^{-1}$ is assigned to the N–H vibration of PANI.

The structural properties are further characterized by the Raman scattering spectroscopy, as shown in Fig. 5(a). The Raman band at $\sim$1169 $cm^{-1}$ is attributed to the C–C stretching/C–H in plane bending of the synthesized layered PANI nanosheets [27]. The observation of Raman band at $\sim$1371 $cm^{-1}$ is assigned to the presence of C$\sim$N$^{\bullet+}$ (where '$\sim$' denotes an intermediate bond between a single and a double) stretching mode of the delocalized polaronic charge carriers in PANI [28]. Moreover, the Raman bands at $\sim$1494 and $\sim$1587 $cm^{-1}$ is associated to N–H bending/C–H bending of benzenoid and C=C (Quinoid)/C–C (benzenoid) stretching respectively [29]. The corresponding Raman mapping images in the two ranges of $\sim$1300–1400 $cm^{-1}$ and $\sim$1550–1600 $cm^{-1}$ are depicted in Fig. 5(b,c). The Raman mapping in the range of 1300–1400 $cm^{-1}$ (Fig. 5(b)) shows the scattered light blue color on the major blue area of mapping, which might present the C$\sim$N$^{\bullet+}$ stretching modes (Raman shift at $\sim$1371 $cm^{-1}$) of delocalized polaronic charge carriers in PANI

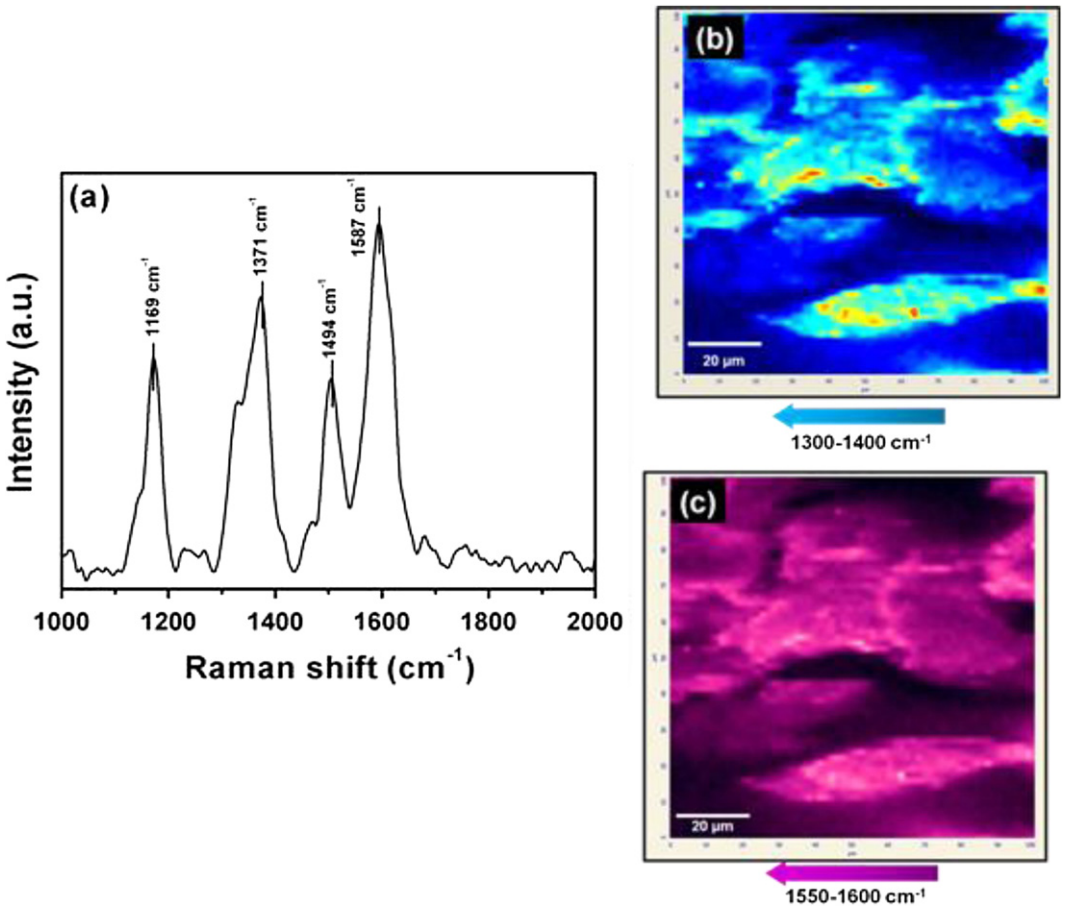


**Fig. 5.** Raman scattering spectrum (a) and its corresponding Raman mapping in 1300–1400 $cm^{-1}$ (b) and in 1550–1600 $cm^{-1}$ (c) of layered PANI nanosheets.

backbone. However, uniform distribution of the C=C (Quinoid)/C–C (benzenoid) stretching in layered PANI nanosheets are observed in the range of 1550–1600 $cm^{-1}$, as shown in Fig. 5(c). Thus, the uniformly distributed C=C/C–C bonding along with $C\sim N^{\bullet+}$ bonding in Raman mapping confirms the formation of high quality of layered PANI nanosheets. These results are in an excellent agreement with the FTIR results.

UV–vis and photoluminescence spectroscopy of layered PANI nanosheets are examined to study the absorption and optical properties. From UV–vis spectrum (Fig. 6(a)), the absorbance band at ~274 and ~345 nm are originated from the $\pi$–$\pi^*$ transition of PANI [30–32]. The broader absorption band at ~601 nm is referred to n-$\pi^*$ transition which suggests the polarons formation into the conductive PANI [33]. The room temperature photoluminescence (PL) spectrum of layered PANI nanosheets with an excitation wavelength of ~320 nm is shown in Fig. 6(b). A single broader PL peak at ~452 nm is observed in the blue-green region by the layered PANI nanosheets which is associated with $\pi$–$\pi^*$ transition of the benzenoid unit of PANI [34]. The presence of single PL absorption band in layered PANI nanosheets usually represents the benzenoid or amine group which is subsequently quenched to a quinoid or imine group of PANI [15]. Therefore, no PL band is observed by the quinoid unit of PANI.

### 3.3. Phenol chemical sensor based on layered PANI nanosheets electrode

The electrocatalytic activity of layered PANI nanosheets electrode towards the detection of phenol is examined by the cyclicvoltametry (CV) analysis. Fig. 7 shows the typical CV of layered PANI nanosheets electrode without and with a series of phenol concentrations (20 μM–0.32 mM) in 0.1 M phosphate buffer (pH=7.0) at the scan rate of 100 $mVs^{-1}$. The layered PANI nanosheets electrode shows the relatively low redox current in the absence of phenol, as shown in Fig. 7(a). Importantly, the prominent oxidation peak with the maximum anodic current of $\sim 1.1\times10^{-4}$ A at ~0.37 V is obtained with the addition of lowest phenol concentration (20 μM), indicating the significant sensing response and high electrocatalytic activity over the surface of layered PANI nanosheets. The weak reduction peak with low cathodic current of $-4.67\times10^{-5}$ A is also observed in the CV curve. The electrochemical behavior with prominent oxidation peak along with weak reduction peak is quite similar to the reported literatures [35] and thus, the following reaction could be proposed for phenol (Scheme 1).

A series of CV plots have been carried out with various phenol concentrations ranging from 20 μM–0.32 mM in 0.1 M PBS to further examine the electrochemical properties of layered PANI nanosheets electrode. Fig. 7(b) shows the typical quasi-reversible redox peaks to the electrochemical reaction of layered PANI nanosheets electrode towards the phenol chemical in PBS. The oxidation peak is gradually increased with the increase of phenol concentration from 20 μM–0.32 mM. It is reported that the high height of oxidation peak and the high anodic current are referred to the faster electron-transfer reaction in the electrochemical system via high electrocatalytic behavior of the working electrode [36]. The highest anodic current is obtained at the highest concentration of phenol (0.32 mM), which is about 2 times larger than the lowest phenol concentration 20 μM. The

considerable increased of the anodic current demonstrates that the electrochemical activity of layered PANI nanosheets electrode is remarkably promoted for the detection of phenol chemical and thus, confirms the involvement of high electrons transfer process via high electrocatalytic activity of the electrode.

The electrochemical properties is further elaborated by measuring the electrochemical impedance spectroscopy (EIS) of layered PANI nanosheets electrode in the wide range concentration of phenol ~20 μM–0.32 mM in 0.1 M PBS with the frequency range 100 kHz–1 Hz, as shown in Fig. 8. The depressed semi circle in the high frequency region is observed in all cases which typically define the parallel combination of the charge transfer resistance ($R_{CT}$) of the electrochemical reaction and the double layer capacitance ($C_{dl}$) at the interface of the layered PANI nanosheets film/electrolyte (phenol in PBS) [37]. In general, the diameter of the large semicircle in EIS plot denotes $R_{CT}$ which is related to the redox reaction of phenol. The $R_{CT}$ of electrode also depends on the dielectric and insulating features at the electrode/electrolyte interface [38]. Herein, the $R_{CT}$ values of layered PANI nanosheets electrode has decreased with the increase of phenol concentration in PBS. The order of $R_{CT}$ values of layered PANI nanosheets electrode with different phenol concentrations are as ~38.29 kΩ (20 μM) < ~24.95 kΩ (40 μM) < ~8.98 kΩ (60 μM) < ~6.72 kΩ (80 μM) < ~3.38 kΩ (0.16 mM) < ~2.83 kΩ (0.32 mM). It is known that large $R_{CT}$ leads the slow charge transfer rate of the electrochemical system [39]. In our case, at highest phenol concentration (0.32 mM) the layered PANI nanosheets electrode obtains the lowest $R_{CT}$ value, which indicates the high sensing response towards phenol in the electrochemical system. This result is in good agreement with CV observations.

The fabricated phenol chemical sensor is illustrated in Fig. 9(a), which is comprised of layered PANI nanosheets electrode as working electrode and Pt wire as cathode electrode in PBS. The measurement of current (I)–voltage (V) characteristics (Fig. 9(b)) is performed for evaluating the sensing properties such as sensitivity, detection limit and correlation coefficient of layered PANI nanosheets electrode towards phenol chemical. After the addition of phenol (20 μM), the sudden increase in the current of ~67.3 μA is observed by the fabricated phenol chemical sensor however, a low current (~11.1 μA) is recorded without phenol based chemical sensor. A series of the *I–V* characteristics have been established to elucidate the sensing parameters of the fabricated phenol chemical sensor with layered PANI nanosheets electrode, as shown in Fig. 9(b). It is seen that the current has continuously increased with the increase of the phenol concentrations (~20 μM–0.32 mM), suggesting the good sensing response toward the phenol chemical by the layered PANI nanosheets electrode based phenol chemical sensor. This phenomenon might originate by the generation of large number of ions and the increase of ionic strength of the solution with the addition of different concentration of phenol. A calibration curve of current versus phenol concentration (Fig. 9(c)) is plotted to calculate the sensitivity of the fabricated phenol chemical sensor.

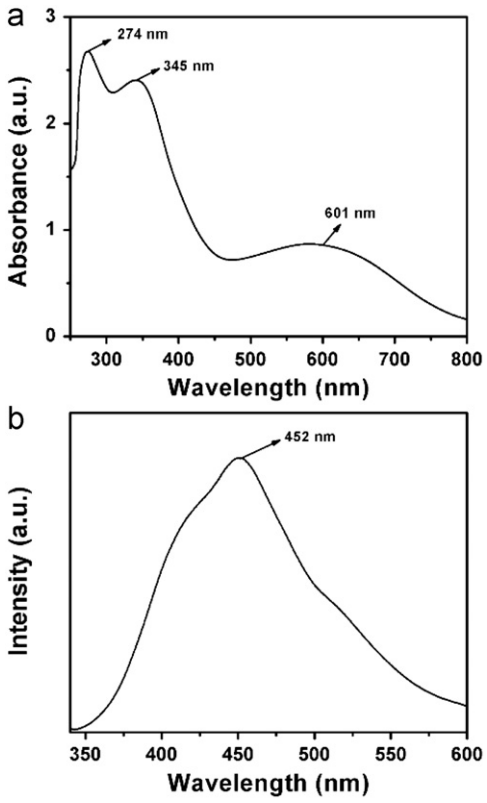


**Fig. 6.** UV–vis (a) and PL spectra (b) of layered PANI nanosheets.

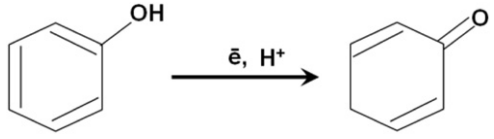


**Scheme 1.** Mechanism of phenol during the electrochemical reaction.

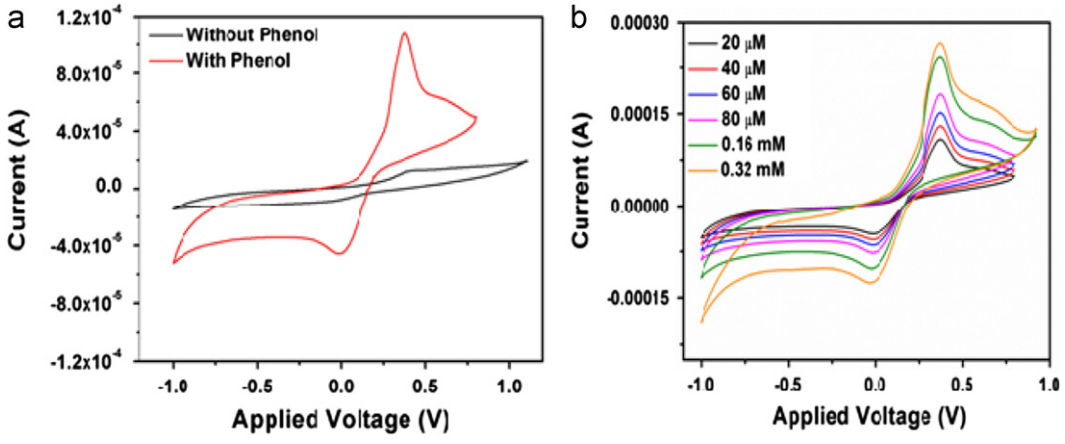


**Fig. 7.** (a) Typical cyclovoltametry curve of fabricated phenol chemical sensor based layered PANI nanosheets electrode without and with phenol (20 μM) in 10 ml of 0.1 M PBS solution and (b) CV sweep curves in phenol concentrations of 20 μM–0.32 mM in 10 ml of 0.1 M PBS solution.

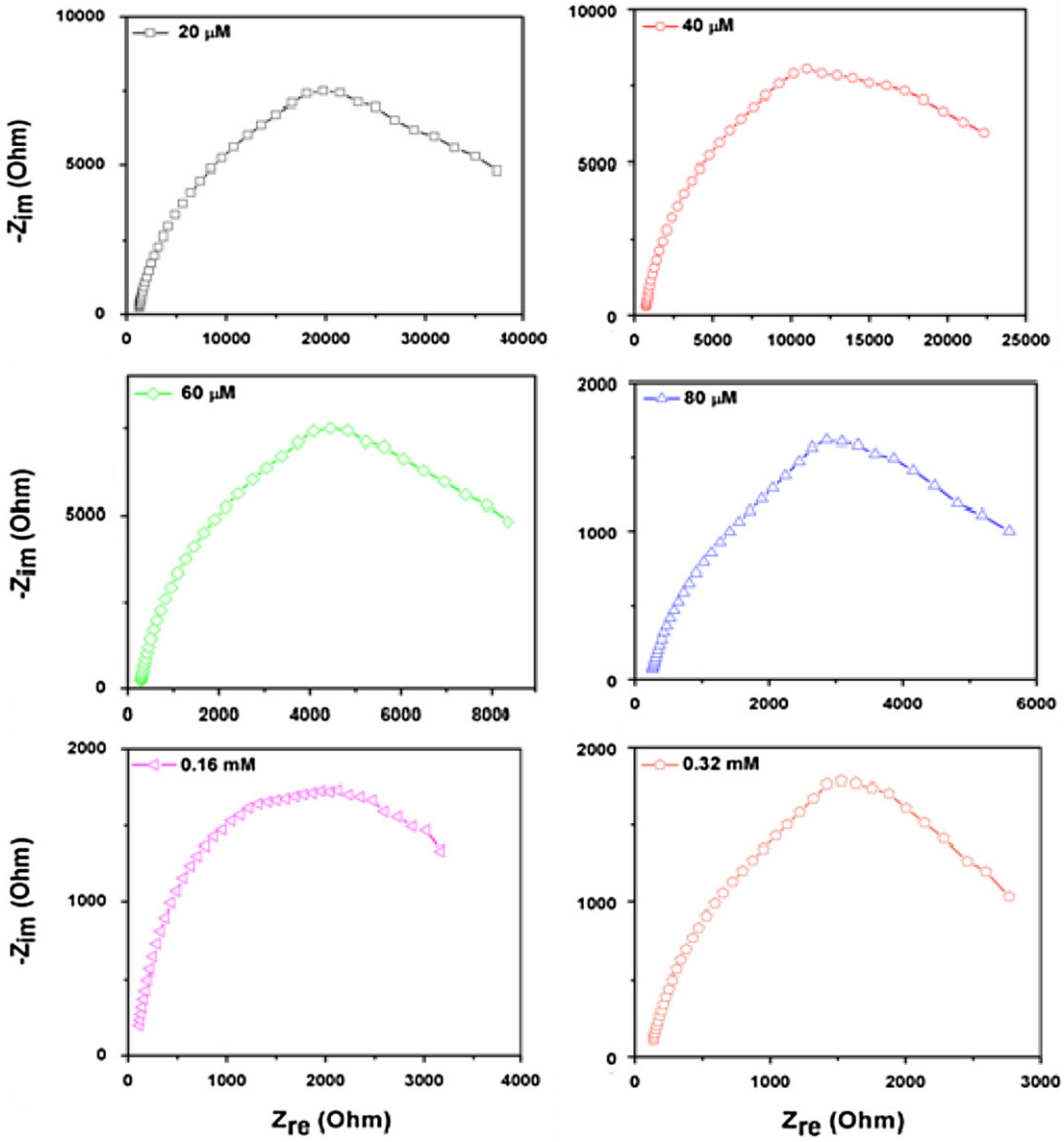


**Fig. 8.** EIS plots of layered PANI nanosheets based electrode in 10 ml of 0.1M PBS solution with different concentrations of phenol.

The calibrated current linearly increases up to the increase of the phenol concentrations ~80 μM and then attains a saturation level in the calibrated plot. The occurrence of the saturation point might due to the unavailability of free active sites over the layered PANI nanosheets electrode for phenol adsorption at higher concentration (>80 μM). The fabricated phenol chemical sensor with layered PANI nanosheets electrode achieves high, and the reproducible sensitivity of ~1485.3 μA $mM^{-1}$ $cm^{-2}$ and the detection limit of ~4.43 μM with correlation coefficient (R) of ~0.9981 and short response time (10 s). A good linearity in the range of 20 μM–80 μM is detected by the fabricated phenol chemical sensor with layered PANI nanosheets electrode. However, the layered PANI nanosheets electrode shows less sensing response towards catechol chemical with the sensitivity of ~41.4 μA $mM^{-1}$ $cm^{-2}$ and the detection limit of 19.4 μM, as shown in Fig. 10. The sensitivity toward catechol chemical with layered PANI nanosheets electrode is comparable to other catechol sensor [42]. For reproducibility and the stability of fabricated phenol chemical sensor, the sensing response by the *I–V* characteristics is measured for three consecutive weeks. It is found that the fabricated phenol chemical sensor did not show any significant decrease in the sensing parameters or properties, which deduces the long term stability of the fabricated phenol sensor based on layered PANI nanosheets electrode. Herein, the achieved sensitivity, detection limit and the correlation coefficient of the fabricated phenol chemical sensor are superior to those of reported literatures on phenol sensor with PANI electrodes, as summarized in Table 1 [40–42]. Thus, the unique layered morphology of PANI nanosheets is promising and effective as working electrode for the detection of phenol chemical.

## 4. Conclusions

The layered PANI nanosheets are synthesized by the chemical polymerization of aniline monomer in the presence of hydrochloric acid and ammonium persulphate at 5 °C for attaining the reliable sensing properties towards the hazardous phenol chemical. From the FESEM and AFM characterizations, the layered nanosheets morphology of synthesized PANI is visibly recorded. The Raman spectra and the Raman mapping of layered PANI nanosheets depict the uniformly distributed C=C/C–C bonding along with $C\sim N^{\bullet+}$ bonding which confirms the formation of high quality of layered PANI nanosheets. The electrochemical behavior of the layered PANI nanosheets based electrode is demonstrated

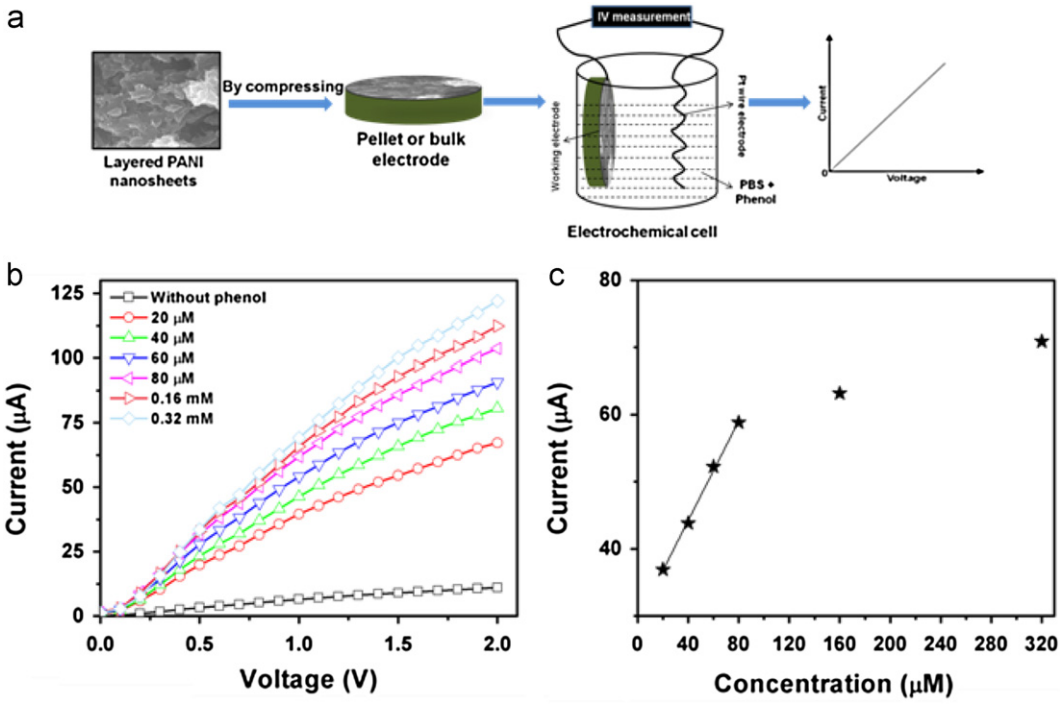


**Fig. 9.** (a) Schematic illustration of the fabricated phenol chemical sensor, (b) *I–V* characteristics of layered PANI nanosheets based phenol chemical sensor at different phenol concentrations (20 μM–0.32 mM) in 10 ml of 0.1 M PBS and (c) the calibration curve of current versus phenol concentration of the fabricated chemical sensor.

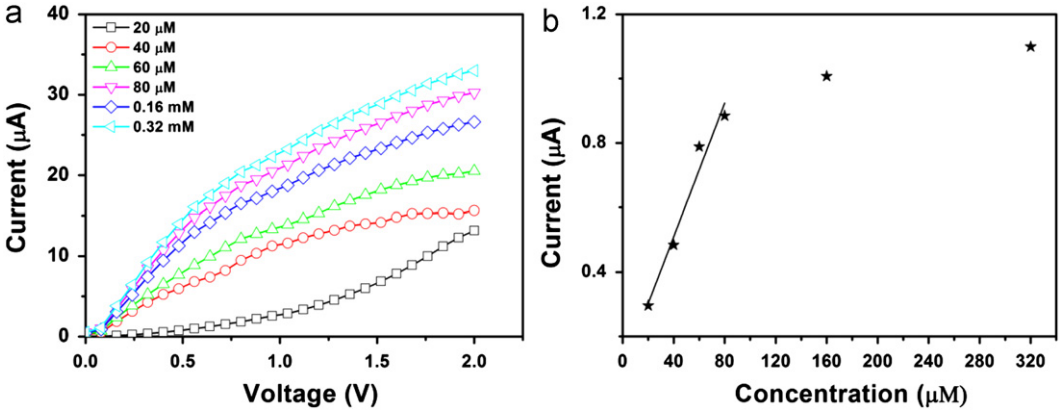


**Fig. 10.** (a) *I–V* characteristics of layered PANI nanosheets based catechol chemical sensor at different catechol concentrations (20 μM–0.32 mM) in 10 ml of 0.1 M PBS and (b) the calibration curve of current versus catechol concentration of the fabricated chemical sensor.

**Table 1**
Sensing response characteristics of various electrodes to phenol chemical.

| Electrode | Limit of detection (μM) | Linearity (μM) | Correlation coefficient | Sensitivity ($\mu A\ mM^{-1}\ cm^{-2}$) | Refs. |
|---|---|---|---|---|---|
| Pan-PAN/PPO electrode[a] | – | 0.1–75 | 0.999 | 960 | [42] |
| Tyrosinase based electrode | 13.7 (nM) | 0–0.629 | 0.9981 | 0.256–0.005 (mC/μM) | [41] |
| GR-PANI/GCE[b] | 0.065 | 0.2–20; 20–100 | 0.9987 | 177.6; 604.2 ($\mu A\ mM^{-1}$) | [40] |
| Layered PANI sheets electrode | 4.43 μM | 20–80 | 0.9981 | 1485.3 | This work |

[a] PAn-PAN = polyaniline–polyacrylonitrile composite electrode.
[b] GR-PANI = graphene-polyaniline composite electrode.

by the electrochemical impedance spectroscopy (EIS) and cyclovoltametry (CV) measurements. The layered PANI nanosheets electrode shows reasonably good electrocatalytic activity towards the detection of phenol chemical, which results from the high redox current and low $R_{CT}$. The current–voltage (*I–V*) characteristics are used to elucidate the sensing parameters of the fabricated phenol chemical sensor with layered PANI nanosheets electrode. The fabricated phenol chemical sensor with the layered PANI nanosheets electrode significantly attains the high sensitivity of $\sim$1485.3 $\mu A\ mM^{-1}\ cm^{-2}$ and the detection limit of $\sim$4.43 μM with correlation coefficient ($R$) of $\sim$0.9981 and short response time (10 s).

## Acknowledgments

This paper is fully supported by the Research Funds of Chonbuk National University in 2012. This work is also supported by NRF Project #2011-0029527. M.S. Akhtar acknowledges the Research Funds of Chonbuk National University in 2011. Korea Basic Science Institute, Jeonju branch is acknowledged, for utilizing the research supported facilities. We would like to thank Mr. Kang Jong-Gyun, Center for University-Wide Research Facilities, Chonbuk National University for his cooperation in TEM images.

## References

[1] S.G. Burton, Curr. Org. Chem. 7 (2003) 1317–1331.
[2] D. Perićin, V. Krimer, S. Trivi, L. Radulovi, Food Chem. 113 (2009) 450–456.
[3] S.C. Atlow, L.B. Aporo, A.M. Klibanov, Biotech. Bioeng. 26 (1984) 599–603.
[4] S. Bashir, J.L. Liu, Sen. Actuators B: Chem. 139 (2009) 584–591.
[5] R.A. King, B.L. May, D.A. Davies, A.R. Bird, Anal. Biochem. 384 (2009) 27–33.
[6] A. Kovacs, A. Kende, M. Mortl, G. Volk, T. Rikker, K. Torkos, J. Chromatogr. A 1194 (2008) 139–142.
[7] X. Ye, L.J. Tao, L.L. Needham, A.M. Calafat, Talanta 76 (2008) 865–871.
[8] S. Morales, R. Cela, J. Chromatogr. A 896 (2000) 95–104.
[9] M. Hasani, M. Moloudi, J. Hazard. Mater. 157 (2008) 161–169.
[10] (a) W.C. Yang, A.M. Yu, Y.Q. Dai, H.Y. Chen, Anal. Lett. 33 (2000) 3343–3353; (b) M. Abaker, G.N. Dar, A. Umar, S.A. Zaidi, A.A. Ibrahim, S. Baskoutas, A. Al-Hajry, Sci. Adv. Mater. 4 (2012) 893–900.
[11] S. Ameen, M.S. Akhtar, M. Husain, Sci. Adv. Mater. 2 (2010) 441–462.
[12] S. Virji, J. Huang, R.B. Kaner, B.H. Weiller, Nano Lett. 4 (2004) 491–496.
[13] Shumaila, G.B.V.S. Lakshmi, M. Alam, A.M. Siddiqui, M. Zulfequar, M. Husain, Sci. Adv. Mater. 4 (2012) 227–231.
[14] K. Lee, S. Cho, S.H. Park, A.J. Heeger, C.W. Lee, S.H. Lee, Nature 441 (2006) 65–68.
[15] S. Ameen, M.S. Akhtar, Y.S. Kim, H.S. Shin, Chem. Eng. J. 181–182 (2012) 806–812.
[16] S. Manigandan, A. Jain, S. Majumder, S. Ganguly, K. Kargupta, Sens. Actuators B: Chem. 133 (2008) 187–194.
[17] S. Ding, D. Chao, M. Zhang, W. Zhang, J. Appl. Poly. Sci. 107 (2008) 3408–3412.
[18] P. Alexander, O. Nikolay, K. Alexander, S. Galina, Prog. Polym. Sci. 28 (2003) 1701–1753.
[19] S. Ameen, M.S. Akhtar, H.S. Shin, Sens. Actuators B: Chem. 06 (2012) 065, http://dx.doi.org/10.1016/j.snb.
[20] A.L. Kukla, Yu.M. Shirshov, S.A. Piletsky, Sens. Actuators B: Chem. 37 (1996) 135–140.
[21] Y. Bo, H. Yang, Y. Hu, T. Yao, S. Huang, Electrochim. Acta 56 (2011) 2676–2681.
[22] P. Kunzo, P. Lobotka, M. Micusik, E. Kovacova, Sens. Actuators B: Chem. 171–172 (2012) 838–845.
[23] P. Wang, M. Liu, J. Kan, Sens. Actuators B: Chem. 140 (2009) 577–584.
[24] J. Zhang, J. Lei, Y. Liu, J. Zhao, H. Ju, J. Zhang, J. Lei, Y. Liu, J. Zhao, H. Ju, Biosen. Bioelect. 24 (2009) 1858–1863.
[25] (a) Z. Dai, G. Wei, X. Xinghu, C. Hongyuan, Chin. Sci. Bull. 51 (2006) 19–24; (b) S. Hasim, S.C. Raghavendra, M. Revanasiddappa, K.C. Sajjan, M. Lakshmi, M. Faisal, Bull. Mater. Sci. 34 (2011) 1557–1561.
[26] S. Ameen, M.S. Akhtar, Y.S. Kim, O.B. Yang, H.S. Shin, J. Nanosci. Nanotech. 11 (2011) 3306–3313.
[27] A.K. Rai, S. Kumar, A. Rai, Vib. Spectrosc. 42 (2006) 397–402.
[28] M. Grzeszczuk, R. Szostak, Solid State Ionics 157 (2003) 257–262.
[29] S. Ameen, M.S. Akhtar, Y.S. Kim, H.S. Shin, Appl. Catal. B: Environ. 103 (2011) 136–142.
[30] X. Zhang, G. Yan, H. Ding, Y. Shan, Mater. Chem. Phys. 102 (2007) 249–254.
[31] S. Ameen, S.G. Ansari, M. Song, Y.S. Kim, H.S. Shin, Superlatt. Microstructures 46 (2009) 745–751.
[32] S. Ameen, M.S. Akhtar, S.G. Ansari, O.B. Yang, H.S. Shin, Superlatt. Microstructures 46 (2009) 872–880.
[33] D. Han, Y. Chu, L. Yang, Y. Liu, Z. Lv, Colloids Surf. A: Physicochem. Eng. Aspects 259 (2005) 179–187.
[34] J.Y. Shimano, A.G. MacDiarmid, Synth. Met. 123 (2001) 251–262.
[35] M. Del, P.T. Sotomayor, A.A. Tanaka, L.T. Kubota, J. Electroanal. Chem. 536 (2002) 71–81.
[36] A. Umar, M.M. Rahman, S.H. Kim, Y.B. Hahn, Chem. Commun. (2008) 166–168.
[37] P. Fiordiponti, G. Pistoia, Electrochim. Acta 34 (1989) 215–221.
[38] R. Khan, A. Kaushik, P.R. Solanki, A.A. Ansari, M.K. Pandey, B.D. Malhotra, Anal. Chim. Acta 616 (2008) 207–213.
[39] M.A. Vorotyntsev, J.P. Badiali, G. Inzelt, J. Electroanal. Chem. 472 (1999) 7–19.
[40] Y. Fan, J.-H. Liu, C.-P. Yang, M. Yu, P. Liu, Sens. Actuators B: Chem. 157 (2011) 669–674.
[41] J. Adamski, P. Nowak, J. Kochana, Electrochim. Acta 55 (2010) 2363–2367.
[42] H. Xue, Z. Shen, Talanta 57 (2002) 289–295.